Case Studies in Construction Materials 19 (2023) e02327

Contents lists available at ScienceDirect

Case Studies in Construction Materials

journal homepage: www.elsevier.com/locate/cscm

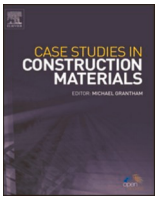

Permeation grouting of low-permeability silty sands with colloidal silica

Gang Liu [a,1], Mingzhi Zhao [a,2], Tengfei Wang [b,*,3], David P. Connolly [c], Yuquan Cai [d], Junsong Jiang [a], Wen Bai [e]

[a] School of Architecture and Civil Engineering, Xihua University, Chengdu 610039, China
[b] MOE Key Laboratory of High-speed Railway Engineering, Southwest Jiaotong University, Chengdu 610031, China
[c] School of Civil Engineering, University of Leeds, Leeds LS2 9JT, UK
[d] Chengdu Cultural Relics Information Center, Chengdu 610072, China
[e] Nouryon Chemicals (Guangzhou) Co. Ltd., Guangzhou 510765, China

ARTICLE INFO

Keywords:
Permeation grouting
Colloidal silica
Nano-silica
Grout injectability
Ground improvement
Chemical additive grouting

ABSTRACT

Permeation grouting is used to fill the voids in soils with particulates for the purpose of improving soil strength. The technique has been predominatly used for cohesionless soils, however due to nanotechnological advancements in colloidal silica, its application to other soil types has more recently gained attention. Given sands with high silt fractions are a common geotechnical deposit, permeation grouting using colloidal silica is potentially an attractive improvement technique, yet has received limited attention. Therefore, this paper seeks to investigate the transport properties of colloidal silica in low-permeability silty sand, in terms of the effective grouting penetration range and peak strength. To this end, permeation injection is applied on low-permeability silty sand in a laboratory setting and then direct shear tests are undertaken. The results indicate colloidal silica concentrations should be greater than 10% to meet water resistance and strength requirements, while lower than 30% to ensure a uniform distribution of grout and adequate penetration. A low injection pressure of between 45 and 55 kPa, and between 65 and 75 kPa, is found to be suitable for permeating 20% and 30% concentrations of colloidal silica, respectively. After 7 days of curing time, silty sand at natural moisture content and treated with a 20% concentration of colloidal silica shows an increase in peak strength of between 58.1% and 78.4%, which increases further with curing time. A 20% concentration of colloidal silica is recommended for treating silty sand with a coefficient of permeability in the range 10^{-6} m/s, based on both injection range and peak strength after treatment. These findings may guide the practice of permeation grouting for low-permeability soils.

1. Introduction

Soil stabilization is commonly performed to enhance the engineering performance of earth structures [1,2]. The methods most

* Corresponding author.
E-mail address: w@swjtu.edu.cn (T. Wang).
[1] ORCID: 0000-0002-1346-9532
[2] ORCID: 0000-0001-6048-0884
[3] ORCID: 0000-0003-4079-0687

https://doi.org/10.1016/j.cscm.2023.e02327
Received 15 March 2023; Received in revised form 13 June 2023; Accepted 19 July 2023
Available online 22 July 2023

commonly utilized in engineering practice are compaction [3,4], such as vibration, dynamic, blast, pile, and replacement [5,6]. However, such traditional methods are usually energy-intensive and often unsuitable for existing sites [7,8]. Moreover, an emerging demand is that the stabilization should be as non-distructive as possible with the soil structure remaining intact during and after soil stabilization [9]. Under these circumstances, passive site stabilization was introduced as an innovative technique to enhance the soil's mechanical properties with minimal disturbance to the soil's skeleton and overlying existing structures [10–12].

Permeation grouting is a type of grouting method in which a low-viscosity additive is injected into soil voids at pressures low enough to not significantly affect the soil's skeleton [13]. Binders are usually penetrated into the soil mass and transported to the desired location, forming a rigid gel to improve the strength properties of the treated soils. Permeation grouting is commonly applied in ground treatment and slope stabilization. Unlike jet or fracture grouting, it requires strict limits on injection pressure and flow rate that are determined by soil permeability and grout rheology. Traditional additives commonly used in permeation grouting include microfine cement, bentonite, sodium silicate, and resins [14,15]. Microfine cement, with a particle diameter usually around 9 μm, is only applicable for permeation through medium to coarse sand. Alternatively, although bentonite, sodium silicate, and resins can fill fine to silty sand pores due to their small partile diameters, controlling their gelling speed for seepage through the interparticle spaces is challenging [16].

As a solution, colloidal nano-silica has become a promising additive [17]. Studies have demonstrated that the introduction of colloidal silica can fill pore spaces and impede particle rearrangement, resulting in enhanced shear strength and reduced soil deformation [18,19]. The bond between the gelled silica and soil particles can also suppress pore water pressure generation, significantly mitigating liquefaction risks for liquefiable sand [20–23]. Colloidal silica has been successfully employed to stabilize underground soil and prevent liquifaction beneath runways and ducts [24]. Additionally, colloidal silica has been used to stabilize landslides, enhancing slope resistance to weathering and increasing strength properties, thereby preventing the formation of landslides [25]. Furthermore, colloidal silica has demonstrated an ability to reduce soil permeability and remediate environmental contaminants [26].

Typically, permeation grouting with colloidal silica is executed on sand possessing a coefficient of permeability surpassing 10^{-5} m/s. However, scant attention has been paid to the permeation grouting of sand characterized by a substantial silt fraction and a coefficient of permeability with magnitudes of 10^{-6} m/s or 10^{-7} m/s. This study aims to develop effective permeation grouting techniques for silty sand utilizing colloidal silica. Through conducting grouting tests with varying concentrations of colloidal silica, it examines the relationships between injectability, zone of injection, and injection pressure. In addition, the peak strength of the silty sand after treatment is compared to untreated samples to assess the efficacy of different colloidal silica concentrations. Recommendations are given regarding the optimum concentration of colloidal silica for permeation grouting of low-permeability silty sands.

2. Background

The process of permeation grouting relies on the properties of soil voids and the rheological properties of additives, making it imperative to maintain strict control over injection parameters such as pressure and flow rate [27]. The feasibility of permeation grouting, also known as injectability, is determined by the density, permeability, and type of soil, as well as the rheological properties

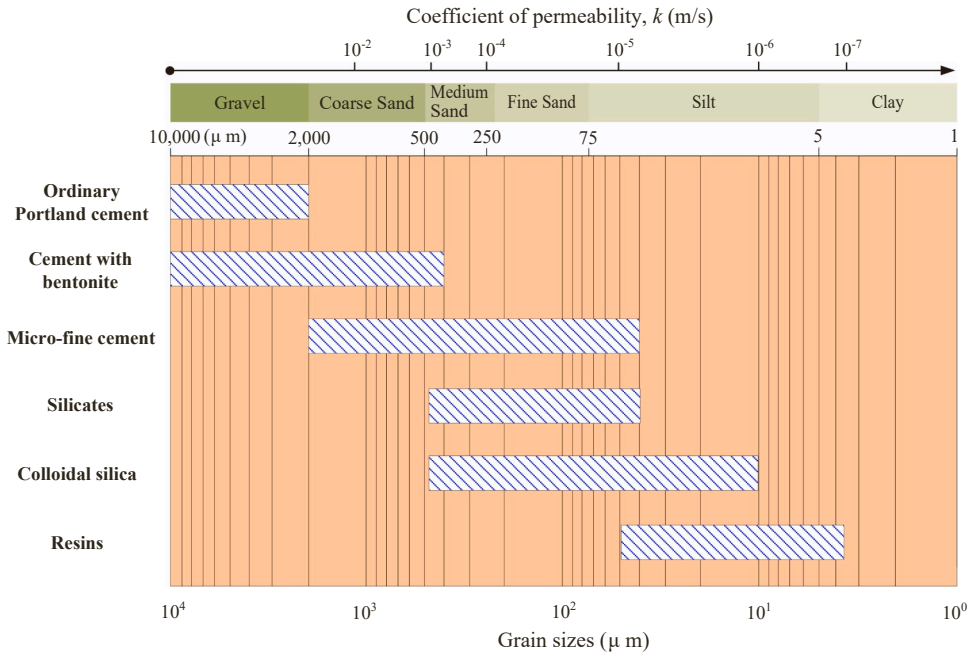

Fig. 1. Applicable range of additives for permeation grouting.

of the grout. To assess the injectability, several empirical equations have been proposed based on Terzaghi's filter criteria for suspensions. One representative equation is [28]:

$$N = \frac{d_{10,soil}}{d_{95,grout}} > 8 \quad (1)$$

where $d_{10,soil}$ and $d_{95,grout}$ are the grain sizes corresponding to 10% soil and 95% grout passing percent, respectively. When N is greater than 8, permeation grouting is feasible. In addition to Eq. 1, other equations have also been proposed in accordance with filter criteria and expressed in a similar form, however with differing grain sizes and N values [29–31].

Terzaghi's filter criteria, while useful for suspension-type grouts, is not practical for solution-type grouts. To address this limitation, injectability can also be expressed in terms of soil permeability [32]. In this context, the soil's coefficient of permeability is a critical factor in assessing injectability [33]. Unlike the filter criteria, the permeability criteria is applicable to both filter- and solution-type grouts, and has broader applicability. However, permeation grouting is a complex process affected by multiple factors, including injection pressure, flow rate, and grout rheological properties [34–38]. Therefore, in situ or laboratory tests are necessary for site-specific applications. Despite this, since injectability is necessary to be evaluated theoretically in the preliminary design stage of a grouting program, the permeability criteria is the first choice to make selection of the grout and determine the critical injection parameters.

Guidelines for evaluating injectability have been proposed for solution-type grouts, taking into account the coefficient of permeability of the treated soil, as shown in Fig. 1 [27,39]. Theoretically, colloidal silica can be used to permeate medium to silty sand with a coefficient of permeability that ranges from 10^{-3} m/s to 10^{-6} m/s, and it presents advantages over most traditional binders in terms of transport properties through sand.

In situ and laboratory studies have investigated the permeation characteristics of colloidal silica through soil, as listed in Table 1. In pratice, when using on sand, colloidal silica typically uses a coefficient of permeability varing from 10^{-5} m/s to 10^{-3} m/s, which is greater than the theoretical value. On the other hand, 'silty sand' rather than 'sand' is more commonly encountered in engineering practice. The presence of a high content of silt in silty sands often leads to a coefficient of permeability as low as 10^{-7} m/s to 10^{-5} m/s, presenting challenges for the successful implementation of permeation grouting.

Despite this, it has been shown theorecally feasible to perform permeation grouting with colloidal silica through low-permeability silty sand [27]. This has sparked interest in developing permeation grouting techniques that can overcome the low permeability limit of silty sand. Colloidal silica, an economical and practical alternative to traditional grouts, has been shown to have excellent strengthening effects on soils. Nonetheless, studies on permeation grouting of silty sand with low permeability using colloidal silica remain scarce. Additionally, the relationship between injection pressure, zong of injection, and colloidal silica concentration is relatively unexplored.

3. Laboratory testing

In this section, a series of laboratory injection tests were conducted to examine the transport properties of colloidal silica through low-permeability silty sand. The grouting system was designed and the injection pressure, volume, and zone were measured for varying concentrations of colloidal silica. The efficacy of the treatment was assessed using the direct shear test to gauge the increase in soil strength.

Table 1
Studies on permeation grouting by means of colloidal silica.

The treated soil			Colloidal silica		Injection pressure (kPa)	Ref.
Soil type	Density (g/ cm^3)	Permeability coefficient (m/s)	Concentration (%)	Accelerator		
Fine sand	1.68–1.72	6.4×10^{-4}	—	Calcium salt	50–300	Delfosse-Ribay et al.[40]
Sand/ Silty sand	—	8×10^{-5} to 5×10^{-4}	30	Sodium chloride	75–150	Gallagher et al. [41]
Sand/ Silty sand	1.46–1.62	2.6×10^{-5} to 2.2×10^{-3}	5	Sodium chloride, hydrochloric acid	N/A	Gallagher and Lin [33]
Fine to silty sand	—	—	8	Sodium chloride	300–500	Rasouli et al.[24]
Sand	—	5×10^{-5} to 2.5×10^{-4}	3–10	Sodium chloride	N/A	Salvatore et al. [16]
Sand	—	5.2×10^{-4}	6, 10	Sodium chloride	5–10	Vranna et al.[42]
Sand/ Silty sand	1.34–1.47	2.85×10^{-4} to 7.67×10^{-4}	40	Sodium chloride	3	Fraccica et al.[43]
Sand	1.90–1.97	2.0×10^{-5}	4, 5, 9	Sodium chloride	90	Conlee et al.[23]
Sand / Sand-Silt mixtures	—	2.01×10^{-7} to 1.19×10^{-4}	15, 40	Sodium chloride	10–100	Fraccica et al.[27]

3.1. Materials

A low-permeability silty sand was prepared for permeation. The grain size distribution of silty sand under analysis was measured per the *Standard for Geotechnical Testing Method* (GB 50123–2019) [44], with results presented in Fig. 2. The average particle size d_{50} was 0.09 mm. The uniformity coefficient was 22, and the gradation coefficient was 0.73. The particles with diameter greater than 0.075 mm account for 55.65% by mass.

The initial moisture content of the silty sand was measured to be 1 − 2% using the oven drying method, while its bulk density in-situ was 1.58 g/cm^3. Accordingly, the dry density of the silty sand was computed to be 1.55 g/cm^3. To determine the permeability of the silty sand, the falling head permeameter method was employed. As a result, the coefficient of permeability was determined to be 3.2×10^{-6} m/s, significantly lower than that of most other sand materials previously reported. Nonetheless, permeation grouting remains theoretically viable; however, the injection pressure and grout concentration must be tailored to ensure an even distribution throughout the soil mass.

The grout is a type of colloidal silica created by Nouryon. This particular colloidal silica is manufactured from saturated solutions of silicic acid and is biologically and chemically inert [45]. The dispersion is alkaline and consists of approximately 40% solid by weight, and has a translucent liquid appearance. The discrete silica particles within the dispersion have a slightly rough and spherical shape, with a particle size that ranges from 10 nm to 11 nm. The density of the grout is 1.3 g/cm^3, with an initial viscosity slightly more viscous than water, measured at 19 cP (1 cP = 0.001 Pa·s). When diluted to 20% and 30% concentrations, the viscosities of the grout are 5 cP and 7 cP respectively. This type of colloidal silica was chosen for its high solid content and strength after gelling. It is sodium stabilized, and the amorphous silica in the dispersion carries a negative surface charge in the alkaline environment, causing the silica particles to repel each other. Upon the addition of a sodium salt solution or acid, the gelation process is initiated due to a significant decrease in the repulsive forces between silica particles. During this stage, siloxane bonds develop continuously, connecting the soil particles together and thus improving mechanical properties.

To meet the necessary requirements of permeation grouting, the grout's viscosity must be kept relatively low. As a result, the study necessitated diluting the colloidal silica, which consists of 40% silica by weight, with distilled water. In addition, sodium chloride (NaCl) was utilized as an accelerator to initiate gelation. Fig. 3 displays the relationship between the gelling time and accelerator concentration for colloidal silica with different silica contents. It is seen that the gelling time of colloidal silica decreased with an increase in both colloidal silica and accelerator (NaCl) concentrations. When the NaCl concentration surpassed 1.0%, the gelling time may not have been sufficient for permeation grouting of colloidal silica with 20% and 30% solids by weight. On the other hand, additional soluble salt could dissolve from the silt fraction of the silty sand, potentially hastening the gelling process to a certain extent. Consequently, the concentration of NaCl electrolyte was maintained at 0.5%.

3.2. Grouting system

The permeation system comprises four main constituents: an air compressor to furnish compressed air, a pneumatic controller to modulate air pressure, a hermetic grout storage bucket, and an injection pipe to insert grout into the treated soil, as demonstrated in Fig. 4. The air compressor holds a total volume of 30 L and a gas flow rate of 70 L/min. The maximum pressure provided by the compressor is 700 kPa, which is sufficient for permeation grouting. KTL Instruments Co., Ltd. produces the pneumatic controller that regulates air pressure in the range of 1 kPa to 900 kPa, with an error tolerance of 1%. The grout storage bucket is fitted with a sealed cap and connected to the pneumatic controller to provide a confined space for air pressure to force the grout into the injection pipe.

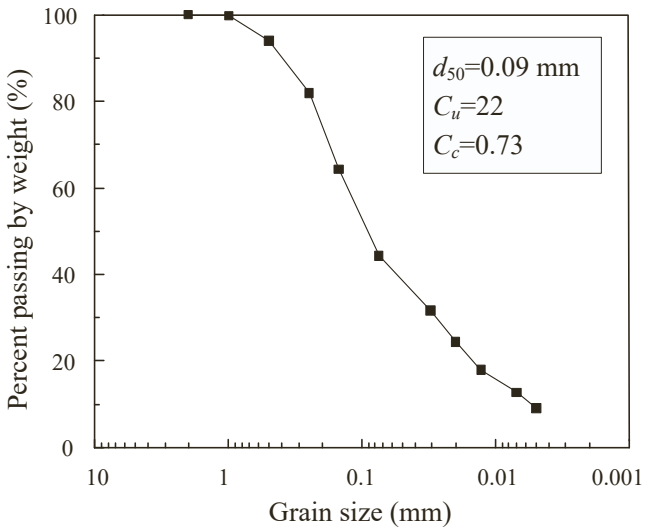

Fig. 2. Grain size distribution of the silty sand under test.

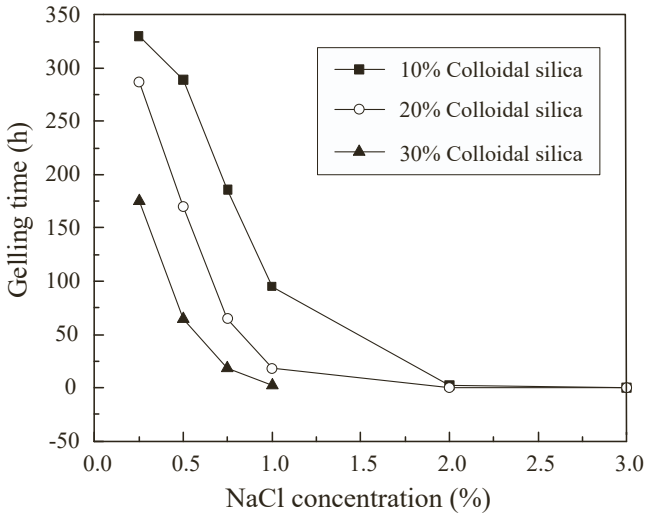

Fig. 3. Gelling time of colloidal silica against accelerator concentration.

The injection pipe utilized in this study measures 500 mm in length, with external and internal diameters of 8 mm and 5 mm, respectively, yielding a pipe wall thickness of 1.5 mm. The pipe's bottom end features a pointed design for effortless insertion into the treated soil. Four grout outlets, with a diameter of 3 mm, are located 150 mm from the bottom and inclined at 90° to one another in the same horizontal plane. A quick-type coupling is positioned at the top end of the injection pipe, facilitating swift connection to the grout guide tube.

Before initiating permeation grouting, a borehole with a diameter of 12 mm is drilled to a depth 10 cm above the desired location, and a suitable amount of water is added to preserve the hole wall. Once water infiltrates the hole wall, the injection pipe is lowered along the borehole, and a sealing putty layer, 10 − 15 cm in length, is enclosed around the upper part of the pipe. The putty layer is secured with tape to preserve its morphology, and the injection pipe is gently hammered to advance another 10 cm to the desired location. This procedure ensures the close combination of the putty layer with the treated soil, preventing grout from effusing along the borehole. After the injection pipe is placed, water is added to the pipe to check for blockages at the grout outlet. If no blockage is found, colloidal silica can be added to the grout bucket. Finally, the air compressor and pneumatic controller can be activated to begin the permeation grouting process, during which the electronic balance measures and records the variation of grout mass.

3.3. Experimental procedure

First an experiment was conducted on silty sand treated with colloidal silica at different concentrations to determine the optimal concentration of colloidal silica. The experiment aimed to balance the fluidity of the grout with the required strength for the treated soil. Colloidal silica was diluted to 10%, 20%, and 30% concentrations and mixed thoroughly with silty sand to form a treated soil with mass ratios of grout to soil of 1:8. Sample columns with a diameter of 39.1 mm and a height of 60 mm were prepared from the treated soils and allowed to gel and cure for 7 d, 14 d, and 28 d. After gelling and curing, the treated silty sand samples were immersed in water for 3 mins. Fig. 5 shows the treated silty sand sample after immersion. The sample treated with 10% colloidal silica concentration nearly collapsed after immersion, while the samples treated with 20% and 30% concentrations remained intact, demonstrating improved water resistance and strength properties of the treated soil with increasing grout concentration. Thus, 20% and 30% concentrations of colloidal silica were selected for the following permeation grouting tests.

Furthermore, the results indicate that the water resistance of the treated silty sand is enhanced with longer curing times at a fixed colloidal silica concentration, underscoring the importance of extending the curing period. However, it should be noted that excessive curing times may lead to limited gains in strength. Research has shown that strength enhancement due to colloidal silica occurs within a range of about four times the time required to reach a resonating gel [46]. Accordingly, typical curing times for colloidal silica range from 7 to 28 d.

Subsequently, the permeation test required the preparation of a silty sand column, achieved by by compacting the sand into an acrylic tube with an 20 cm inner diameter and a 5 mm-thick wall. Standing at a height of 40 cm, this column featured a lower layer of 30 cm, furnished with an initial moisture content of 2%, while the upper 10 cm sustained a greater moisture content of 7%. Acting as a liquid seal, this augmented moisture content in the upper layer hindered grout permeation and surface effusion, a scenario visualized in Fig. 4. An analogous procedure could feasibly be replicated in situ via water infiltration from the surface. The controlled dry density of the silty sand column was 1.55 g/cm^3, resulting in a density of 1.58 g/cm^3 for the lower 30 cm layer and 1.66 g/cm^3 for the upper 10 cm portion. A coefficient of permeability proximate to 3.2×10^{-6} m/s was presumed for the silty sand column, as a consequence of its comparable moisture content and dry density to that of natural silty sand.

In order to ensure the even distribution of grout, permeation tests were carried out with 20% and 30% concentrations of colloidal

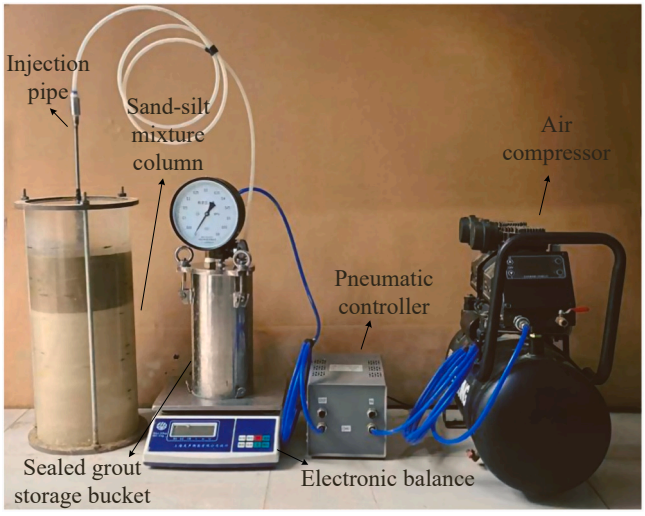

(a)

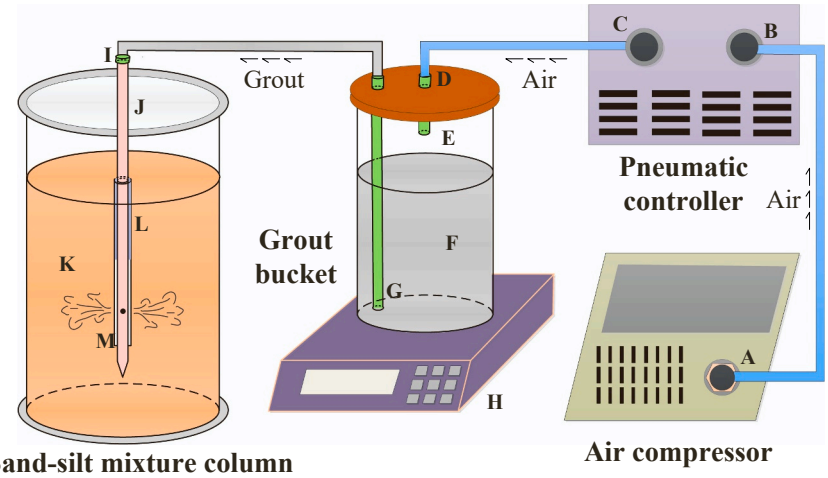

A: Air outlet; B: Air inlet; C: Pressured air outlet; D: Pressured air inlet; E: Compressed air;
F: Levasil CB24; G: Grout inlet; H: Electronic balance; I: Quick coupling;
J: Injection pipe; K: Sand-silt mixture; L: Sealing putty; M: Distributed grout outlet.

(b)

Fig. 4. (a) Photo and (b) schematic of the in-house permeation grouting system.

silica in the silty sand column, while the bulk density and coefficient of permeability remained constant. To avoid damaging the soil structure, an initial injection pressure of 10 kPa was applied during the grouting process. As the flow rate remained below 10 g/min, an additional pressure of 5 − 10 kPa was introduced to expedite the grouting process. To maintain consistent injection pressure, it was necessary to keep the grout flow rate between 10 − 20 g/min. If the flow rate exceeded 20 g/min during the middle or later stage of the permeation grouting, the injection pressure had to be slightly reduced to ensure uniform distribution of the grout in the silty sand mass. The termination of the grouting process warrants certain conditions: (1) the appearance of grout on the tube wall; (2) a reduction in the flow rate to less than 1 g/min; or (3) the surfacing of grout from the silty sand column. Four columns were grouted in total: two treated with 20% concentration and the other two with 30% concentration. Curing times of 7 d and 28 d were tested for each grout concentration, as shown in Table 2.

After the curing process was complete, the treated column was extracted from the acrylic tube to examine the grouting effectiveness. When the silty sand beyond the zone of injection was removed, the soil within the zone remained cohesive and compact due to the cementing effect of the colloidal silica, while the scattered soil lay outside the grouting area. The dimensions of the consolidated soil mass were then measured to determine the effectiveness of the injection.

The use of a cutting ring allowed the collection of undisturbed samples from within the effective grouting area, which was divided

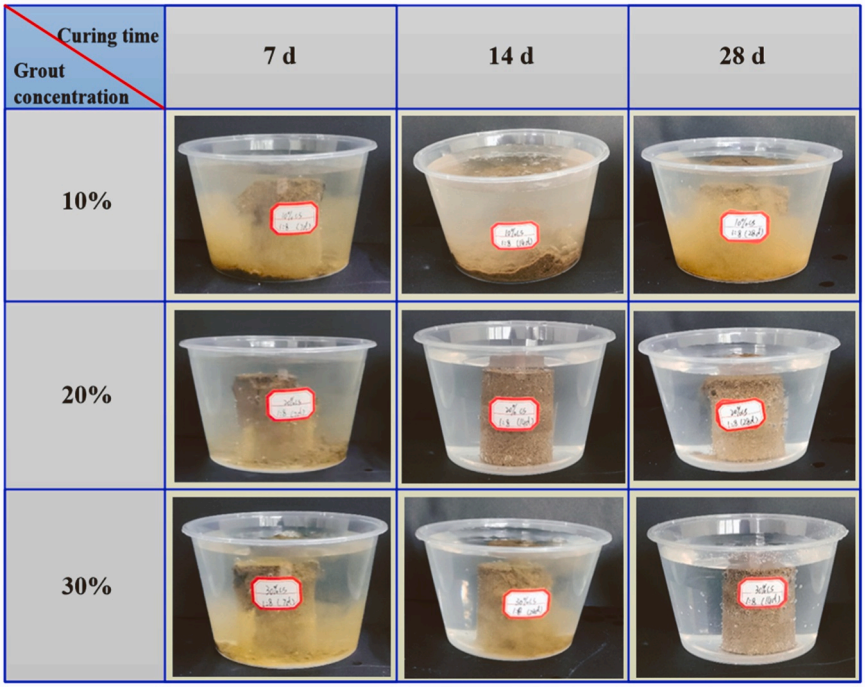

Fig. 5. Treated silty sand samples with different colloidal silica concentrations after immersion.

Table 2
Test program.

Column ID	Grout concentration	Curing time (d)	Sample ID	State during direct shear
1	20%	7	1–1	Natural
			1–2	Immersed
2	20%	28	2–1	Natural
			2–2	Immersed
3	30%	7	3–1	Natural
			3–2	Immersed
4	30%	28	4–1	Natural
			4–2	Immersed

into upper, middle, and lower portions. From each column, six samples were taken, with two from each portion. These samples were grouped into two sets of three, with each set representing the upper, middle, and lower portions. During the direct shear tests, one set of samples remained untreated, while the other was subjected to immersion, as shown in Table 2. The samples were initially consolidated under a normal pressure of 50 kPa before being sheared at a velocity of 0.8 mm/min. The relationship between shear stress and horizontal displacement was then recorded to determine the strength properties of the treated silty sand before and after permeation grouting.

4. Results and analysis

Colloidal silica exhibits the potential to permeate through silty sand with a low injection pressure, and create a significant treatment zone. Furthermore, the treated soil ought to exhibit a substantial rise in peak strength after curing. In this section, the injectability, zone of injection, and enhancement of shear strength in treated soils are used as indicators in establishing the viability of using colloidal silica to stabilize low-permeability silty sand.

4.1. Injectability

During the permeation grouting of the tested columns, the injected grout mass and injection pressure were monitored and recorded against elapsed time as depicted in Fig. 6. Stable injection pressures within the range of 45 – 55 kPa were observed for columns numbered 1 and 2 when treated with 20% concentration of colloidal silica. However, the grouting process was terminated upon the emergence of grout around the tube wall. For the majority of the grouting process, the injected grout mass increased linearly with

elapsed time. The final injected grout masses for Column 1 and 2 were 1379 g and 1343 g, respectively.

Conversely, stable injection pressures for the other two silty sand columns treated with 30% concentration of colloidal silica ranged from 65 kPa to 75 kPa, which is significantly higher than those treated with 20% concentration grout. This implies that grout concentration significantly influences the required injection pressure for permeation grouting. The grouting process was terminated due to the flow rate becoming less than 1 g/min (Column 3) or effusion of grout from the surface of the silty sand column (Column 4). This indicates that a 30% concentration of colloidal silica was difficult to be injected into low-permeability silty sand under a slight injection pressure, and hard to transport through an effective distance to penetrate envenly into the column body. As a result, the final injected grout masses for Column 3 and 4 were only 1081 g and 952 g, respectively, as flow rate of grout becomes tardy or grout effusion occurred prior to arrival at the tube wall. Based on these findings, it can be concluded that for 20% of colloidal silica, the lower injection pressure delivers a greater volume of grout. Thereby 20% of colloidal silica is inclined to have a greater zone of injection penetration compared with 30% grout.

To further explore the injectability of colloidal silica into silty sand, the injected grout mass per unit pressure was calculated for a 10-minute interval. The injected grout per unit pressure was then plotted against elapsed time for the tested columns, as illustrated in Fig. 7. For a 20% concentration grout, the injected grout per unit pressure remained in the range, 1.9 g/kPa to 3.2 g/kPa, for most of the injection period. Conversely, a 30% concentration of grout showed a mass per unit pressure varying from 0.5 g/kPa to 1.7 g/kPa. This suggests that colloidal silica with a 20% concentration can be more easily permeated through silty sand than grout with a 30% concentration.

4.2. Zone of injection penetration

Upon reaching the target curing time, the acrylic tube was removed from the treated columns, as illustrated in Fig. 8. The column treated with 20% concentration grout exhibits a near-cylindrical shape, signifying that the grout was uniformly distributed within the silty sand, with the grout outlets as the central points. The height of Column 1 and 2 are 24.4 cm and 24.8 cm respectively, with diameters of 17.1 cm and 17.5 cm correspondingly. In contrast, columns treated with a 30% concentration do not have regular

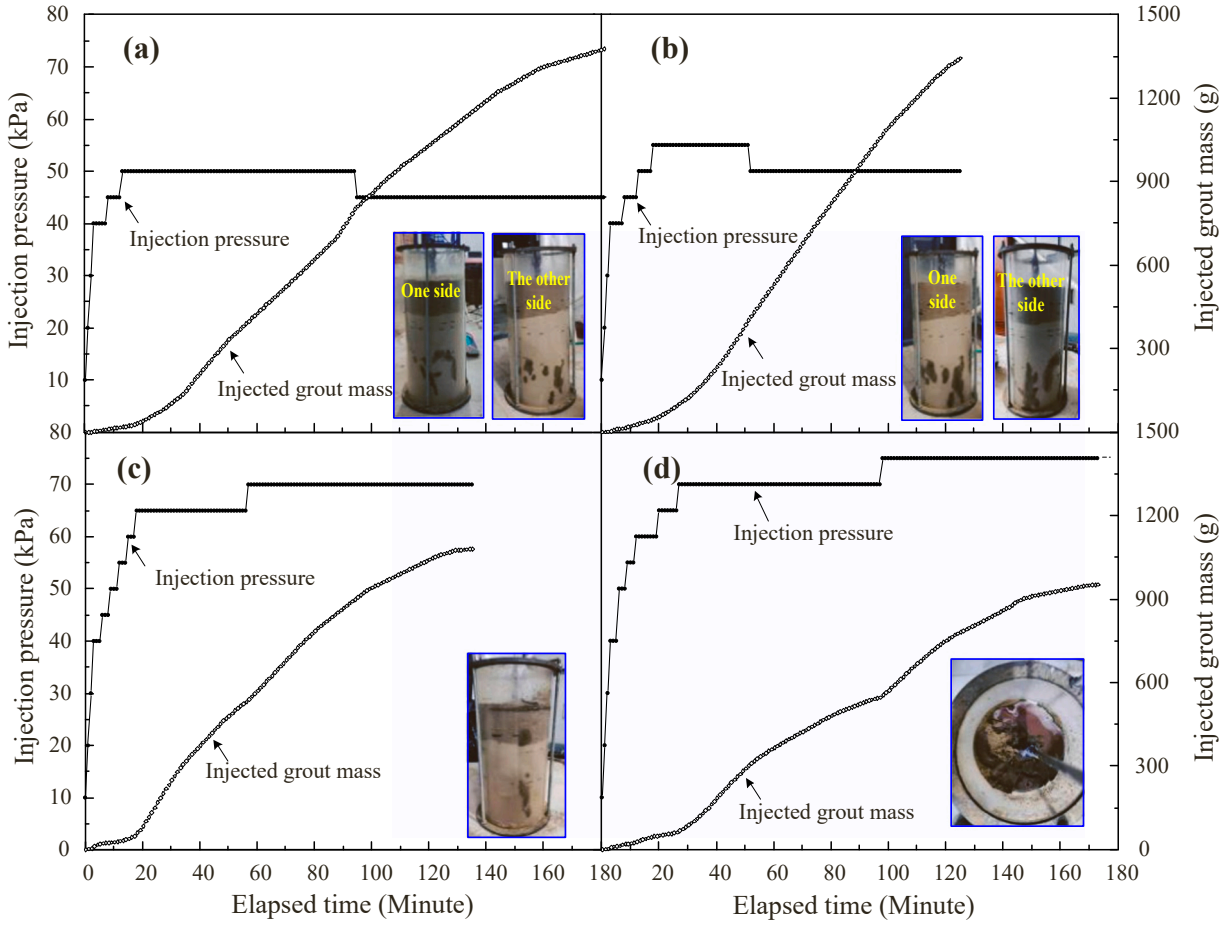

Fig. 6. Injection pressure and grout mass against elapsed time: (a) Column 1; (b) Column 2; (c) Column 3; (d) Column 4.

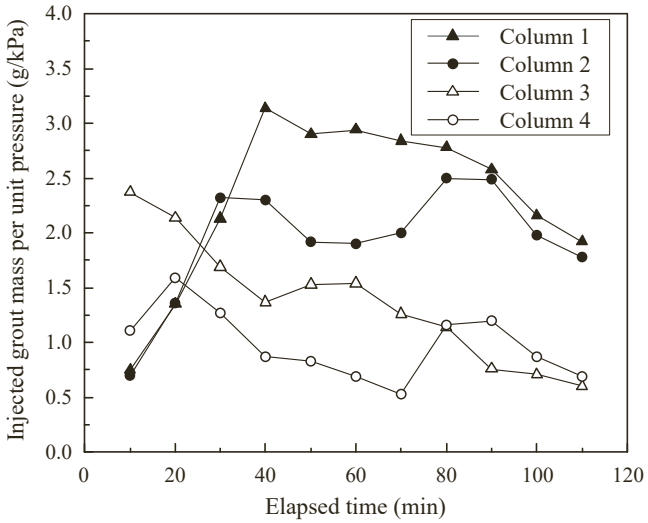

Fig. 7. Comparison of injected grout per unit pressure for colloidal silica with different concentrations.

Fig. 8. The treated silty sand columns with different grout concentrations.

geometric shapes compared to those treated with a 20% concentration. For Column 3, the upper portion is inclined to have a greater diameter than the middle and lower portions, while Column 4 has a larger lower portion compared to the upper and middle portions. The heights of the treated columns are 21.6 cm and 19.2 cm for Columns 3 and 4 respectively, with maximum diameters of 15.6 cm and 15.4 cm. Both the height and diameter of the columns treated with a 30% concentration are smaller than those treated with a 20% concentration, indicating that colloidal silica at a 20% concentration has a greater uniformity of influence in silty sand with a permeability coefficient of the order of 10^{-6} m/s.

To quantify the differences between shapes, a three-dimensional laser scanner (TDLS) was used to record the geometries of the injected silty sand bodies, as depicted in Fig. 9. The volume of the injected silty sand was calculated from this digitized information. Fig. 10 illustrates a comparison of the injected volumes of silty sand using colloidal silica with different concentrations. The columns treated with 20% concentration of colloidal silica had injected volumes of 5436 cm^3 and 5279 cm^3, respectively, with an average of 5357.5 cm^3. However, the average injected volume of silty sand treated with a 30% concentration of grout was only 3081.0 cm^3, which is 42.5% less than that treated with 20% concentration grout. Consequently, it was inferred that a 20% concentration of colloidal silica had a wider field of influence in the low-permeability silty sand compared to the 30% concentration of grout.

Ideally, a cylindrical zone of injection is expected to produce in the silty sand column after colloidal silica treatment. The volume of

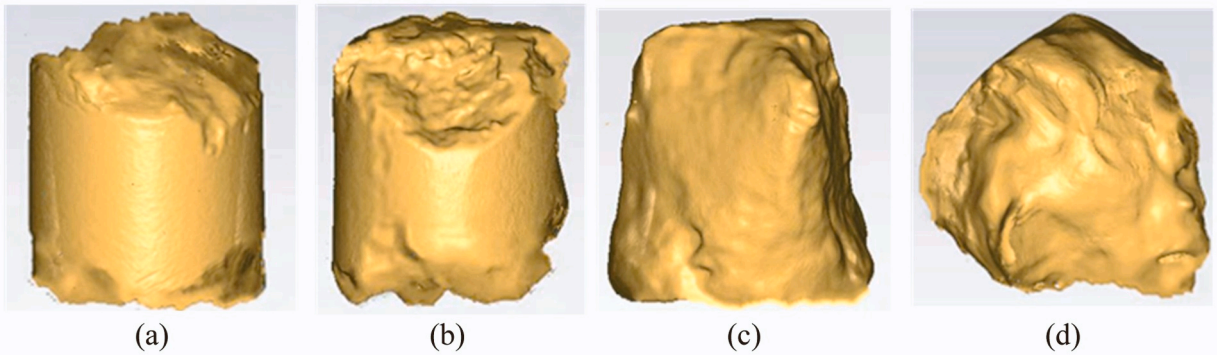

Fig. 9. Digitized model of the treated silty sand columns with a volume of: (a) 5436 cm^3; (b) 5279 cm^3; (c) 3369 cm^3; (d) 2793 cm^3.

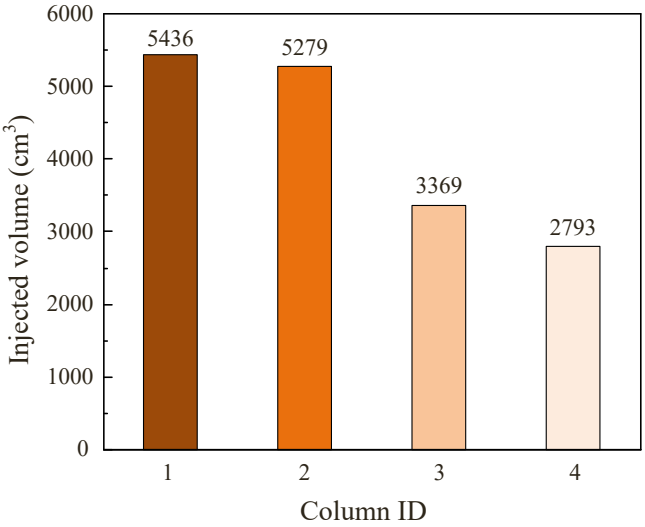

Fig. 10. Volume of the injected silty sand columns.

the cylindrical zones can be calculated with the maximum height and diameter of the treated silty sand columns. Thereby the filling ratio of colloidal silica can then be defined as the ratio of the injected volume obtained from TDLS to the volume of the external cylinder, as presented in Fig. 11. The filling ratio of 20% concentration of colloidal silica averages at 92.8%, which is significantly larger than 79.9%, the averate filling ratio of 30% concentration grout. This implies that the injection and transport of 20% colloidal silica through low-permeability silty sand basically conform with cylindrical filling model, while the treated zone of injection penetration by 30% concentration of colloidal silica presented a greater divergence from the cylindrical model.

4.3. Shear strength

The relationship between shear stress and displacement was plotted for samples with different grout concentrations and curing time, as illustrated in Fig. 12. Fig. 12(a) shows the comparison between the samples treated with 20% colloidal silica versus the untreated samples after 7 d of curing. Both treated and untreated samples exhibit a linear increase in shear stress with displacement in the initial stages, but the stress remains constant after the horizontal displacement reaches a certain level. This indicates that both treated and untreated samples display strain hardening characteristics. In their natural state, the treated samples have peak shear strengths of 52.0 kPa, 48.6 kPa, and 54.9 kPa, respectively, for the upper, middle, and lower portions, which represent an increase of 69.1%, 58.1%, and 78.4% compared to the untreated samples, as shown in Fig. 13. For the samples that were immersed during the direct shear process, the peak strengths of the treated samples increase by 37.4%, 59.2%, and 31.8%, respectively. Therefore, the samples from the upper, middle, and lower portions of the column have peak strengths that are similar. Furthermore, the treated samples with 20% colloidal silica also exhibit larger peak strengths than the untreated samples. This suggests that 20% colloidal silica can provide uniform reinforcement in the soil mass, which can increase the shear strength of silty sand.

Fig. 12(b) illustrates the correlation between shear strength and displacement for samples treated with 20% colloidal silica and cured for 28 d. The treated samples exhibit peak strengths of 66.2 kPa, 61.9 kPa, and 58.0 kPa for the upper, middle, and lower

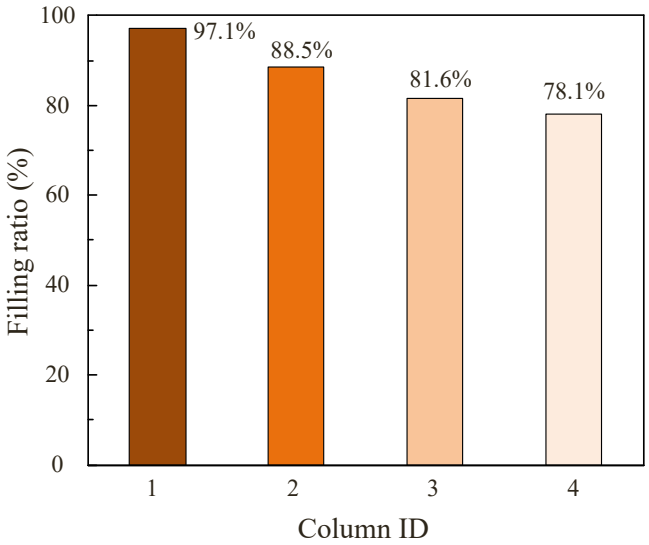

Fig. 11. Fill ratio of colloidal silica in accordance with cylindrical filling model.

portions, respectively. Theses are significantly higher than the untreated samples and surpass the strengths of the samples cured for 7 d. This indicates that the strength of the treated samples increases with the curing time for a given grout concentration. As for the immersed samples, their peak strengths had an average of 28.8 kPa, which is a 49.2% increase. While the strengths of the immersed samples are lower than those of the natural ones, there is still an evident improvement in peak strength after the permeation grouting treatment.

Fig. 12(c) and (d) depict the strength properties of the samples treated with 30% grout concentration and cured for 7 d and 28 d, respectively. It is noteworthy that the treated samples taken from the middle section and kept in their natural state display strain softening features that differ from other samples. Additionally, the peak strengths of the natural middle samples reach up to 83.3 kPa and 92.3 kPa after 7 d and 28 d of curing time, respectively, which are significantly greater than those of the other treated samples. Correspondingly, the peak strengths of the immersed samples extracted from the middle portion are 32.6 kPa and 35.9 kPa after 7 d and 28 d of curing time, respectively, and have the most significant increase compared to the samples collected from the upper and lower portions (Fig. 13). Given that the samples obtained from the middle section have the highest shear strength in both natural and immersed states, it is likely that the grout is not evenly distributed in the silty sand body.

To examine the effects of 30% colloidal silica the peak strengths of treated samples were also investigated. Results show that the peak strengths of natural samples taken from the upper and lower portions are 40.7 kPa and 43.3 kPa after 7 d of curing, and 42.2 kPa and 62.4 kPa after 28 d of curing, respectively. An obervation of note is that the peak strengths of these samples are comparable to or even lower than those treated with 20% colloidal silica. For the immersed samples, a marginal increase in peak strength is observed in those originating from both upper and lower portions, when compared to samples treated with a 20% grout concentration. An exception lies in samples situated near the grout outlet; otherwise, the ascent in peak strengths of treated samples remains inconsequential as grout concentration escalates from 20% to 30%. This is because the higher viscosity of the grout used in the 30% concentration treatment may hinder the uniform distribution of the grout into the soil mass, which could negatively impact the soil strength properties. Therefore, to ensure uniform grout distribution in low-permeability silty sand with a coefficient of permeability at the magnitude of 10^{-6} m/s, we recommend using 20% colloidal silica.

5. Conclusions

To explore the permeation grouting of low-permeability silty sand using colloidal silica at different concentrations, a series of laboratory injection tests and direct shear tests were conducted. The experimental parameters included injection pressure, injected grout volume, diameter of injection influence zone, and peak shear strength of the treated silty sand. From the results, the conclusions were:

- Given the presence of fines in silty sand, the formation of cementation between silica particles can be impeded. Hence, a concentration of colloidal silica greater than 10% is required to attain the desired water resistance and strength properties.
- To penetrate low-permeability silty sand (e.g., permeability coefficient of 10^{-6} m/s), grouting pressure ranging from 10 − 75 kPa can be applied. For the tested column, the flow rate should be controlled between 10 g/min and 20 g/min to avoid grout blockage or damage to the soil structure.

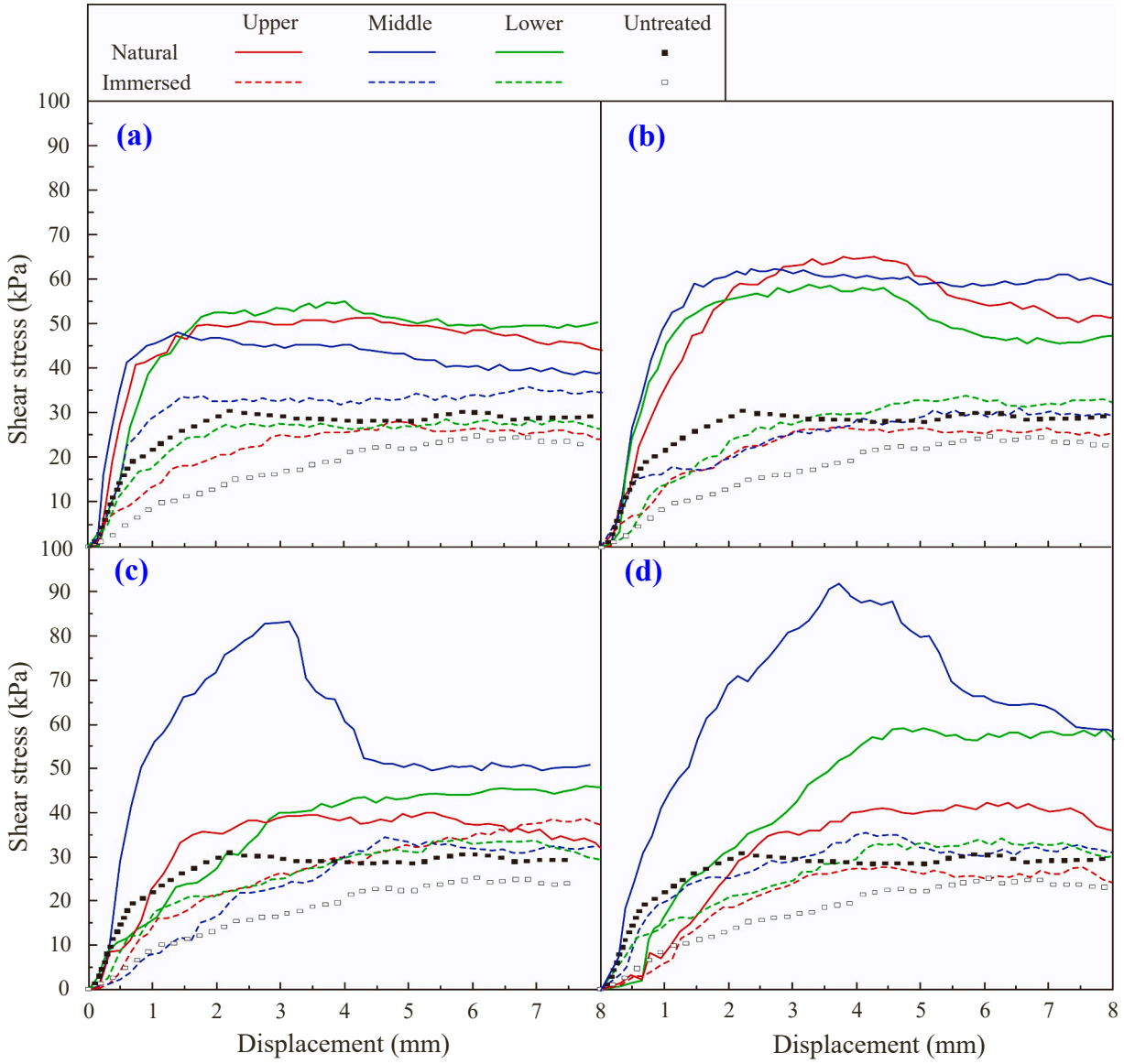

Fig. 12. Relationship between shear strength and displacement for the treated specimens: (a) Column 1; (b) Column 2; (c) Column 3; (d) Column 4.

- A concentration of 30% colloidal silica tends to lead to a narrow injection range and uneven distribution of colloidal silica within the silty sand. Thus, it is recommended to use a grout concentration of 20%, as it provides both a wider near-cylindrical zone of injection penetration and stronger peak strength.
- After a curing period of 7 d, the peak strengths of silty sand at natural moisture content and treated with 20% concentration of colloidal silica increased by 58.1%– 78.4%. This percentage further increased to 88.4%– 115.1% after a curing time of 28 d.

The concentration of colloidal silica selected for permeation grouting of low-permeability silty sand should consider both the transport properties and strength required for the treated soil. Although this study proposed a feasible concentration of colloidal silica for transport through low-permeability silty sand, future investigations could establish a theoretical model for the quantitative evaluation of suitable concentration in terms of transport distance and strength enhancement. Nevertheless, this study provides valuable recommendations for stabilizing low-permeability soils.

Declaration of Competing Interest

The authors declare that they have no known competing financial interests or personal relationships that could have appeared to influence the work reported in this paper.

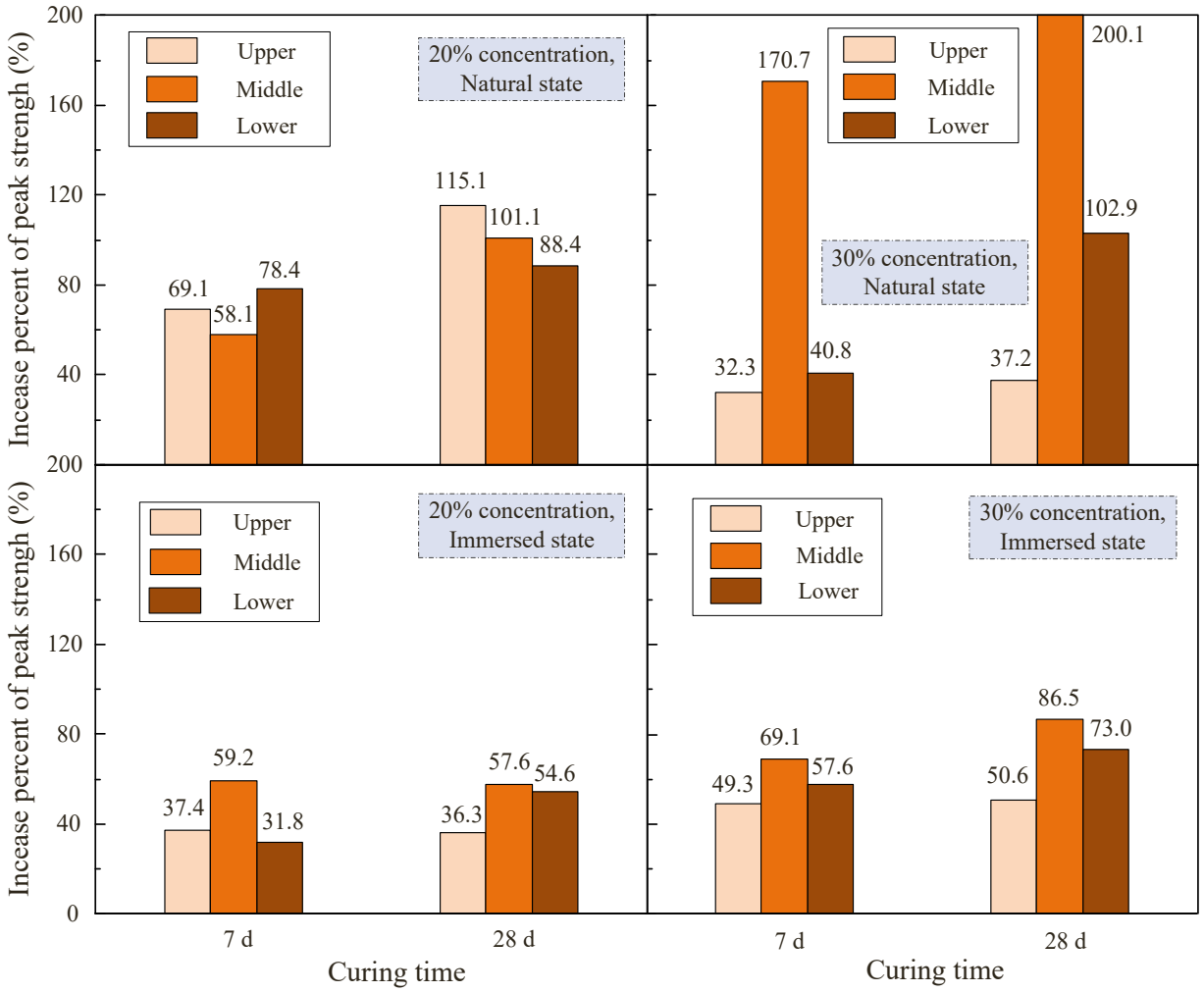

Fig. 13. Percent increase of peak shear strength for the treated samples with different concentrations of colloidal silica.

Data Availability

Data will be made available on request. The data presented in this study are available on request from the corresponding author.

Acknowledgments

This research was funded by the National Natural Science Foundation of China (grant number 52008341) and the Natural Science Foundation of Sichuan Province (grant numbers 2022NSFSC0472, 2022NSFSC1165, and 2023NSFSC0391).

References

[1] Q. Luo, D. Liang, T. Wang, et al., Application of high-vesicularity cinder gravels to railway earth structure in Ethiopia, Journal of Materials in Civil Engineering - ASCE 32 (11) (2020), 04020347.
[2] W. Chen, S. Qu, L. Lin, Q. Luo, T. Wang, Ensemble learning methods for shear strength prediction of fly ash-amended soils with lignin reinforcement, Journal of Materials in Civil Engineering - ASCE 35 (4) (2023), 04023022.
[3] T. Wang, Q. Luo, L. Zhang, et al., Dynamic response of stabilized cinder subgrade during train passage, Construction and Building Materials 270 (2021), 121370.
[4] T. Wang, H. Ma, J. Liu, et al., Assessing frost heave susceptibility of gravelly soils based on multivariate adaptive regression splines model, Cold Regions Science and Technology 181 (2021), 103182.
[5] J. Krishnan, S. Shukla, The utilisation of colloidal silica grout in soil stabilisation and liquefaction mitigation: a state of the art review, Geotech. Geol. Eng. 39 (2021) 2681–2706.
[6] Y. Huang, Z. Wen, Recent developments of soil improvement methods for seismic liquefaction mitigation, Nat. Hazards 76 (3) (2015) 1927–1938.
[7] M. Hamada, Soil Liquefaction and Countermeasures. Engineering for earthquake disaster mitigation. Springer Series in Geomechanics and Geoengineering, Springer, Tokyo, 2014, pp. 125–152.
[8] A. Pamuk, P.M. Gallagher, T.F. Zimmie, Remediation of piled foundations against lateral spreading by passive site stabilisation technique, Soil Dyn. Earthq. Eng. 27 (9) (2007) 864–874.

[9] Q. Luo, P. Wu, T. Wang, Evaluating frost heave susceptibility of well-graded gravel for HSR subgrade based on orthogonal array testing, Transportation Geotechnics 21 (2019), 100283.
[10] P.M. Gallagher, Mitchell J.K. , 2000. Passive site remediation for mitigation of liquefaction risk. In: Proceedings of MEDAT-2 Work MCEER, University of Buffalo, Suny (2000) 149–155.
[11] P.M. Gallagher, S. Finsterle, Physical and numerical model of colloidal silica injection for passive site stabilization, Vadose Zone J. 3 (3) (2004) 917–925.
[12] P.M. Gallagher, A. Pamuk, T. Abdoun, Stabilization of liquefiable soils using colloidal silica grout, J. Mater. Civil. Eng. 19 (1) (2007) 33–40.
[13] J. Han, Principles and Practices Of Ground Improvement, John Wiley & Sons Inc, Hoboken, 2015.
[14] S. He, J. Lai, L. Wang, Ke Wang, A literature review on properties and applications of grouts for shield tunnel, Constr. Build. Mater. 239 (2020), 117782.
[15] G. Spagnoli, A review of soil improvement with non-conventional grouts, Int. J. Geotech. Eng. 15 (3) (2021) 273–287.
[16] E. Salvatore, G. Modoni, M.C. Mascolo, D. Grassi, G. Spagnoli, Experimental evidence of the effectiveness and applicability of colloidal nanosilica grouting for liquefaction mitigation, J. Geotech. Geoenviron. Eng. 146 (10) (2020), 04020108.
[17] Y. Huang, L. Wang, Experimental studies on nanomaterials for soil improvement: a review, Environ. Earth Sci. 75 (6) (2016) 1–10.
[18] C. Wong, M. Pedrotti, G. El Mountassir, R.J. Lunn, A study on the mechanical interaction between soil and colloidal silica gel for ground improvement, Eng. Geol. 243 (2018) 84–100.
[19] P. Persoff, J.A. Apps, G.J. Moridis, 1996. Effect of dilution and contaminants on strength and hydraulic conductivity of sand grouted with colloidal silica gel (No. LBNL-39347; CONF-970208–16). Lawrence Berkeley National Lab.(LBNL), Berkeley, CA (United States), 1996.
[20] P.M. Gallagher, J.K. Mitchell, Influence of colloidal silica grout on liquefaction potential and cyclic undrained behavior of loose sand, Soil Dyn. Earthq. Eng. 22 (9–12) (2002) 1017–1026.
[21] T. Kodaka, Y. Ohno, T. Takyu. Cyclic shear characteristics of treated sand with colloidal silica grout. In Proceedings of the 16th International Conference on Soil Mechanics and Geotechnical Engineering, IOS Press (2005) 401–404.
[22] J.A. Díaz-Rodríguez, V.M. Antonio-Izarraras, P. Bandini, J.A. López-Molina, Cyclic strength of a natural liquefiable sand stabilized with colloidal silica grout, Can. Geotech. J. 45 (10) (2008) 1345–1355.
[23] C.T. Conlee, P.M. Gallagher, R.W. Boulanger, R. Kamai, Centrifuge modeling for liquefaction mitigation using colloidal silica stabilizer, J. Geotech. Geoenviron. Eng. 138 (11) (2012) 1334–1345.
[24] R. Rasouli, K. Hayashi, K. Zen, Controlled permeation grouting method for mitigation of liquefaction, J. Geotech. Geoenviron. Eng. 142 (11) (2016), 04016052.
[25] A.A. Ponomarev, O.V. Zerkal, E.N. Samarin, Protection of the transport infrastructure from influence of landslides by suspension grouting, Procedia Eng. 189 (2017) 880–885.
[26] M.R. Noll, D.E. Epps, C.L. Bartlett, P.J. Chen, 1993. Pilot field application of a colloidal silica gel technology for in situ hot spot stabilization and horizontal grouting. In Proc., 7th National Outdoor Action Conf (1993) 207–219.
[27] A. Fraccica, G. Spagnoli, E. Romero, M. Arroyo, R. Gómez, Permeation grouting of silt-sand mixtures, Transp. Geotech. 35 (2022), 100800.
[28] R.J. Krizek, H.J. Liao, R.H. Borden, Mechanical properties of microfne cement/sodium silicate grouted sand, Geotech. Spec. Publ. 1 (30) (1992) 688–699.
[29] C.L. Huang, J.C. Fan, K.W. Liao, T.H. Lien, A methodology to build a groutability formula via a heuristic algorithm, KSCE J. Civ. Eng. 17 (1) (2013) 106–116.
[30] I.N. Markou, D.N. Christodoulou, E.S. Petala, D.K. Atmatzidis, Injectability of microfine cement grouts into limestone sands with different gradations: experimental investigation and prediction, Geotech. Geol. Eng. 36 (2018) 959–981.
[31] A. Miltiadou-Fezans, T.P. Tassios, Penetrability of hydraulic grouts, Mater. Struct. 46 (10) (2013) 1653–1671.
[32] H. Cambefort, The principals and applications of grouting, Q. J. Eng. Geol. Hydrogeol. 10 (1977) 57–95.
[33] P.M. Gallagher, Y. Lin, Colloidal silica transport through liquefiable porous media, J. Geotech. Geoenviron. Eng. 135 (11) (2009) 1702–1712.
[34] J.F. Raffle, D.A. Greenwood, 1961. The relationship between the rheological characteristics of grouts and their capacity to permeate soils. 5th International Conference on Soil Mechanics and Foundation Engineering, 2 (1961) 789–793.
[35] A. Bodocsi, M.T. Bowers, Permeability of acrylate, urethane and silicate grouted sands with chemicals, J. Geotech. Eng. 117 (1991) 1227–1244.
[36] S. Akbulut, A. Saglamer, Estimating the groutability of granular soils: a new approach, Tunn. Undergr. Space Technol. 17 (4) (2002) 371–380.
[37] M. Pedrotti, C. Wong, G. El Mountassir, J.C. Renshaw, R.J. Lunn, Desiccation behaviour of colloidal silica grouted sand: a new material for the creation of near surface hydraulic barriers, Eng. Geol. 270 (2020), 105579.
[38] G. Spagnoli, S. Collico, Multivariate analysis of a grouted sand with colloidal silica at different dilution stages, Transp. Geotech. 40 (2023), 100987.
[39] X.N. Gong, Handbook for ground treatment, China Architecture and Building Press, Beijing, 2008.
[40] E. Delfosse-Ribay, I. Djeran-Maigre, R. Cabrillac, D. Gouvenot, Factors affecting the creep behavior of grouted sand, J. Geotech. Geoenviron. Eng. 132 (4) (2006) 488–500.
[41] P.M. Gallagher, C.T. Conlee, K.M. Rollins, Full-scale feld testing of colloidal silica grouting for mitigation of liquefaction risk, J. Geotech. Geoenviron. Eng. 133 (2007) 186–196.
[42] A. Vranna, T. Tika, A. Papadimitriou, Laboratory investigation into the monotonic and cyclic behaviour of a clean sand stabilised with colloidal silica, Géotechnique 72 (5) (2022) 377–390.
[43] A. Fraccica, G. Spagnoli, E. Romero, M. Arroyo, R. Gómez, Exploring the mechanical response of low-carbon soil improvement mixtures, Can. Geotech. J. 59 (5) (2022) 726–742.
[44] Ministry of Housing and Urban-Rural Development of People's Republic of China. GB T 50123–2019. Standard for geotechnical testing method. Chinese standard, Beijing, 2019.
[45] R.K. Iler, The chemistry of silica: solubility, polymerization, colloid and surface properties and biochemistry, John Wiley & Sons, New York, NY, 1979.
[46] P.M. Gallagher, Y. Lin, Column testing to determine colloidal silica transport mechanisms. Innovations in grouting and soil improvement, Innov. Grouting Soil Improv. (2005) 1–10.